

Supplementary Figure 1: Podocyte morphology is preserved in naïve ADAM10 Δ pod mice.

Supplementary Figure 2: Podocyte morphology is preserved in naïve ADAM10 Δ pod mice.

Supplementary Figure 3: ADAM10 localization in human glomerular injuries.

Supplementary Figure 4: Glomerular ADAM10 expression increases in APN.

Supplementary Figure 5: Alteration of glomerular morphology is attenuated in APN antibody treated ADAM10 Δ pod mice.

Supplementary Figure 6: Intrinsic mouse IgG deposition does not differ between ADAM10 Δ pod and control littermate mice in APN.

Supplementary Figure 7: Alteration of podocyte structure is attenuated in ADAM10 Δ pod mice in APN.

Supplementary Figure 8: Foot process effacement is attenuated in ADAM10 Δ pod mice in APN nephritis.

Supplementary Figure 9: Cultured murine podocytes exposed to APN antibodies represent a suitable model for the analysis of ADAM10 function.

Supplementary Figure 10: The Notch signaling pathway is not activated in an ADAM10-dependent way in podocytes after exposure to APN-antibodies.

Supplementary Figure 11: Activation of Wnt signaling pathways after exposure to APN-antibodies partially depends on ADAM10 in podocytes.

Supplementary Figure 12: N-cadherin is shed in an ADAM10-dependent manner in cultured murine podocytes.

Supplementary Figure 13: Cell-cell adhesion proteins are expressed at the apical side of developing podocytes.

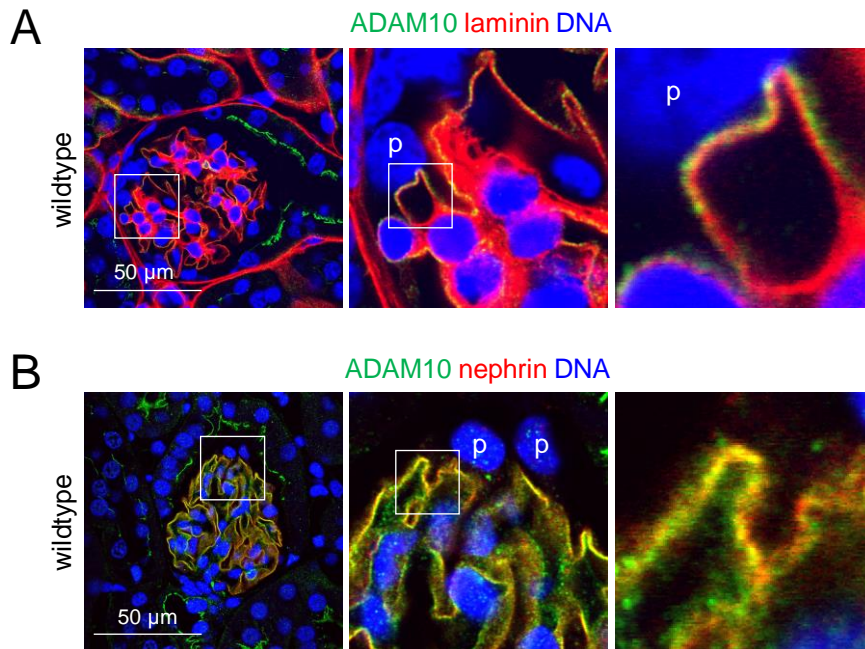
Supplementary Figure 14: P-cadherin expression does not differ between naïve ADAM10 Δ pod and control littermate mice.

Supplementary Figure 15: N-cadherin expression does not differ between naïve ADAM10 Δ pod and control littermate mice.

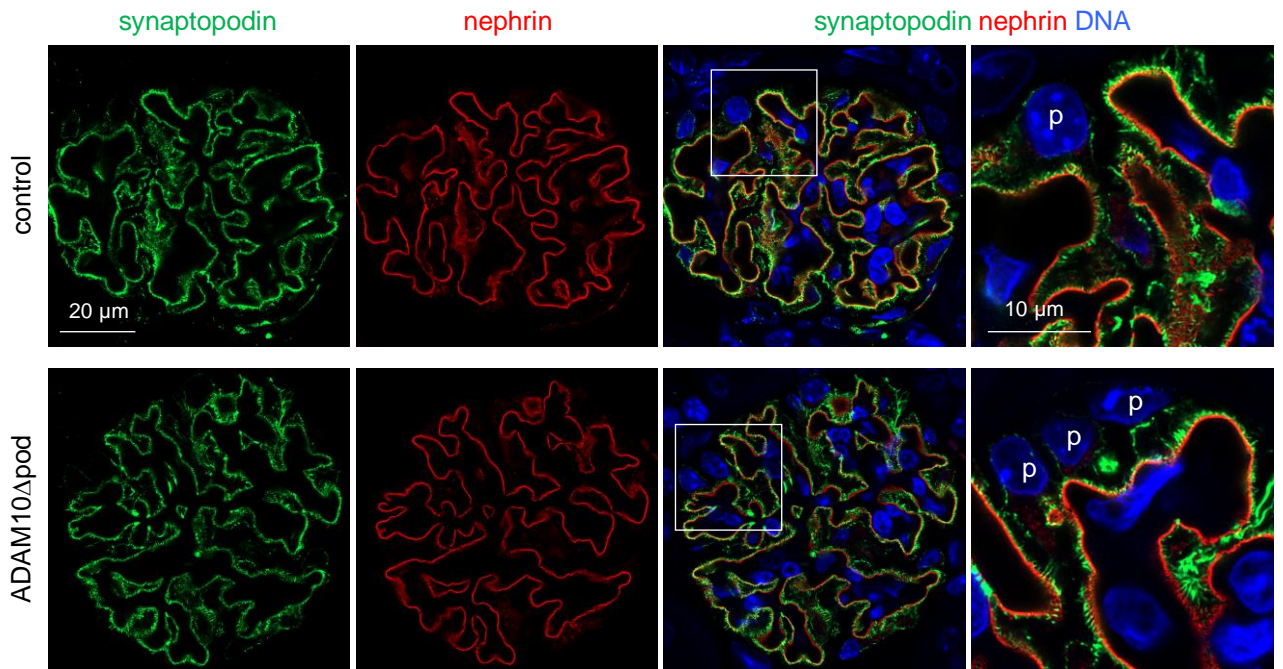
Supplementary Figure 16: β -catenin expression is enhanced in the nuclei and cytoplasm of podocytes in the setting of APN nephritis.

Supplementary Table 1: Oligonucleotide sequences for used for qRT-PCR in cultured murine podocytes and isolated glomeruli.

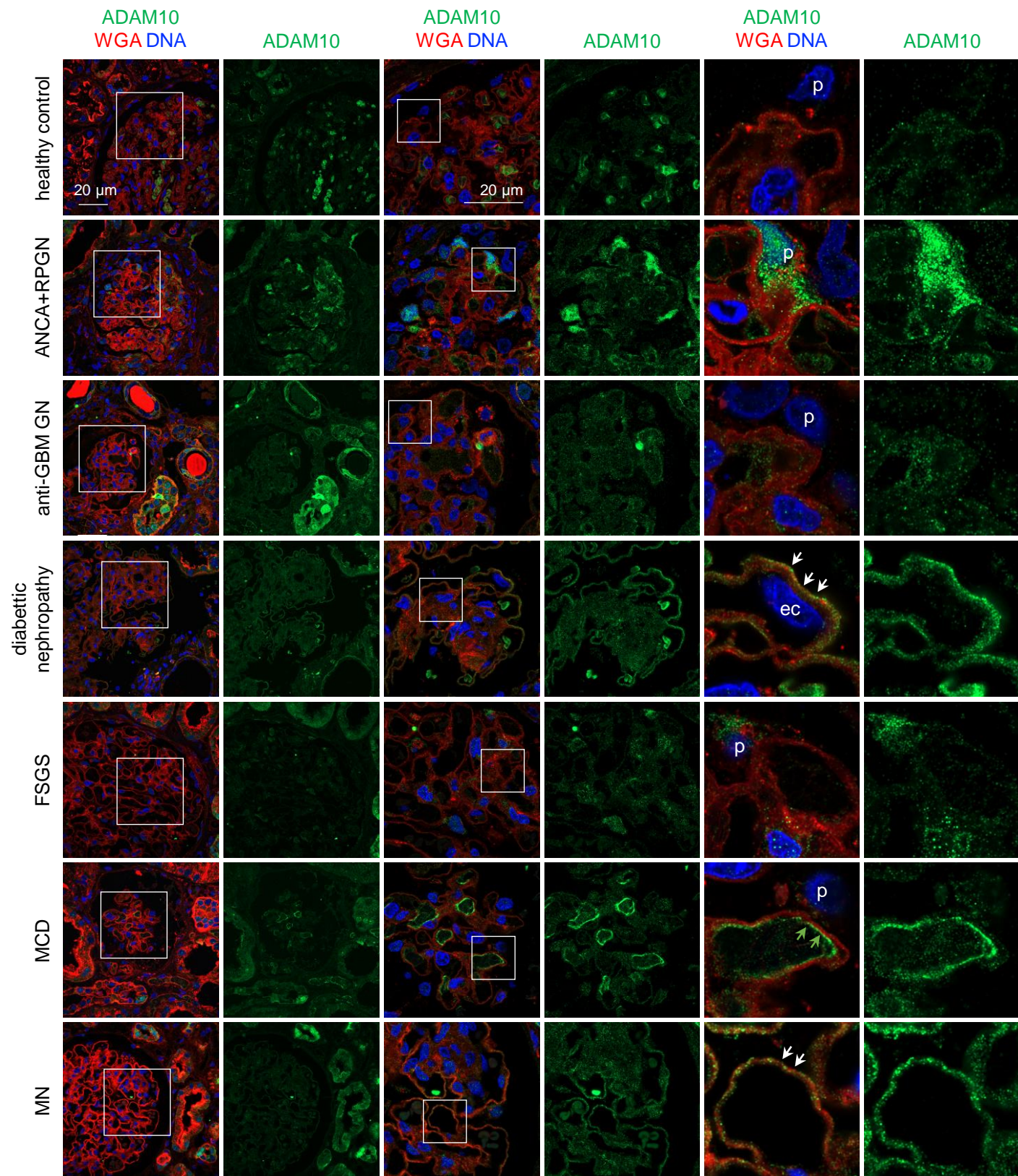
Supplementary Table 2: Summary of the findings regarding ADAM10 regulators in our proteomic datasets.



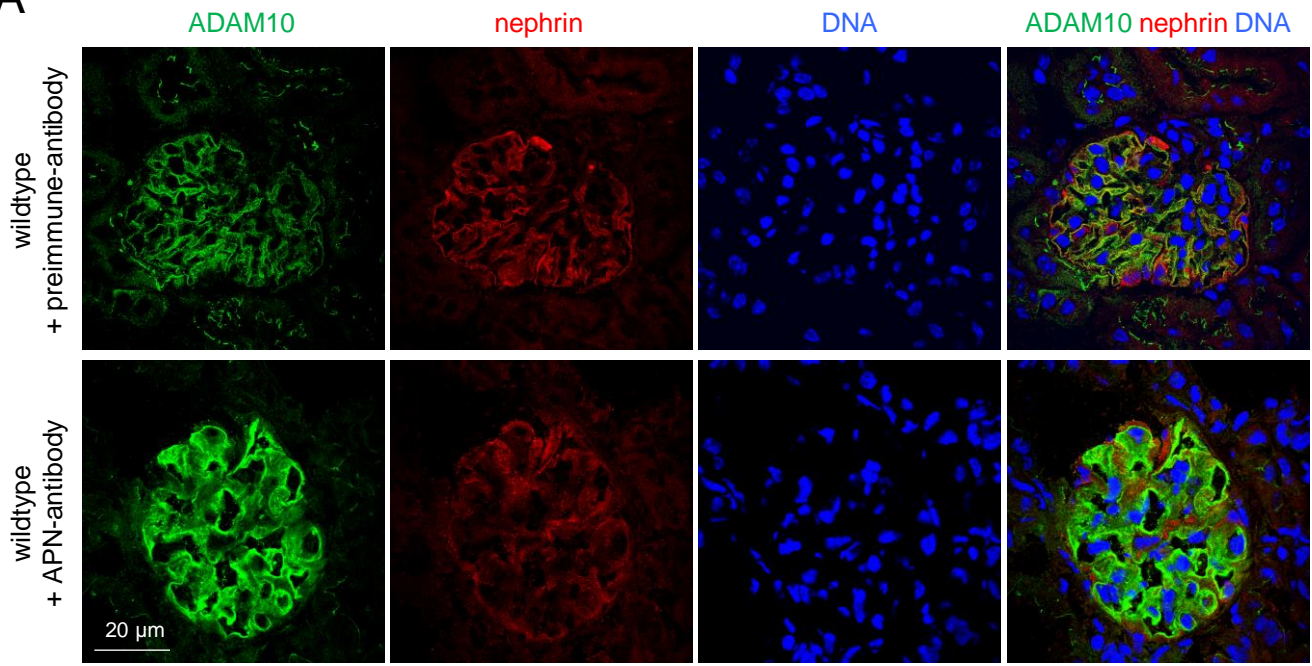
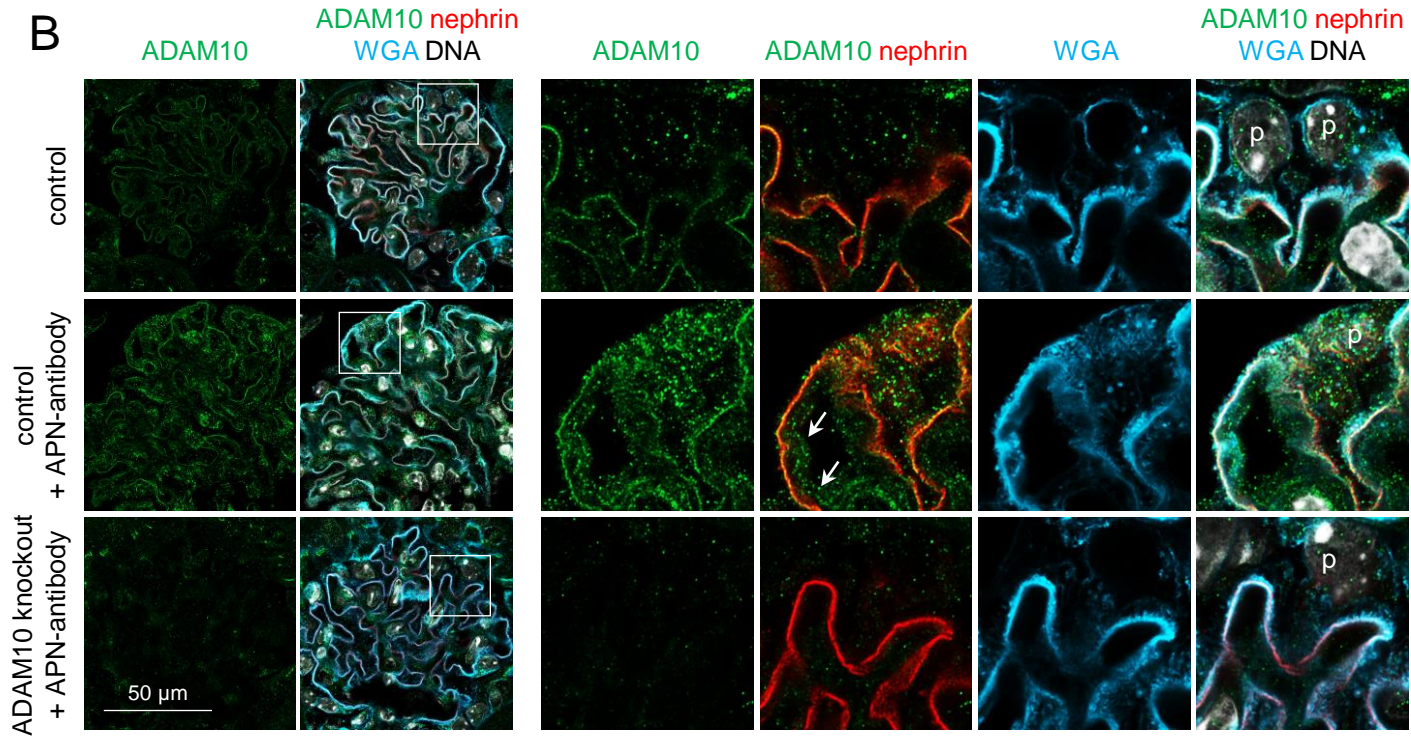
Supplementary Figure 1: Podocyte morphology is preserved in naïve ADAM10 Δ pod mice. Representative confocal images of ADAM10 expression (green) using a rat monoclonal antibody in a C57BL/6 kidney (**A**) in relation to the glomerular basement membrane protein laminin or (**B**) the slit diaphragm protein nephrin both red. DNA is stained in blue (Draq5), p = podocyte.



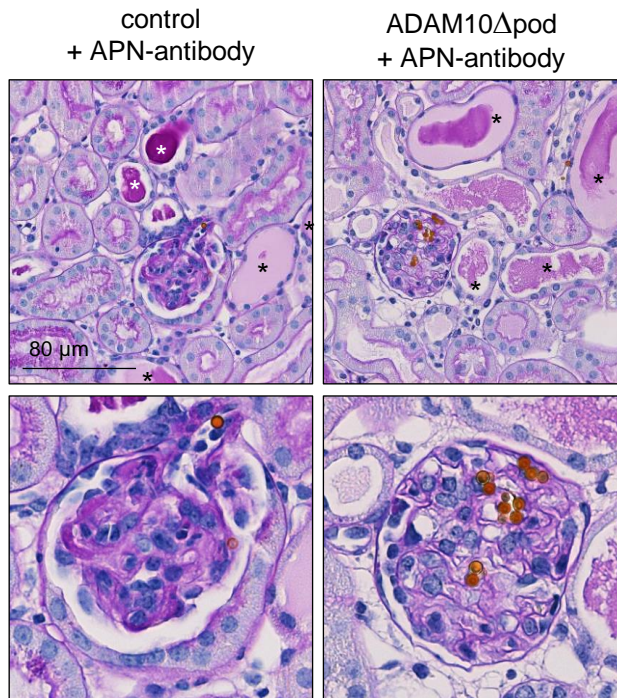
Supplementary Figure 2: Podocyte morphology is preserved in naïve ADAM10 Δ pod mice. Representative high-resolution confocal images of the actin-regulating foot process protein synaptopodin (green) and the slit diaphragm protein nephrin (red), DNA (blue, Hoechst) in podocytes (p). Note the preserved immunolocalization of both proteins in ADAM10 Δ pod mice in comparison to control littermates.



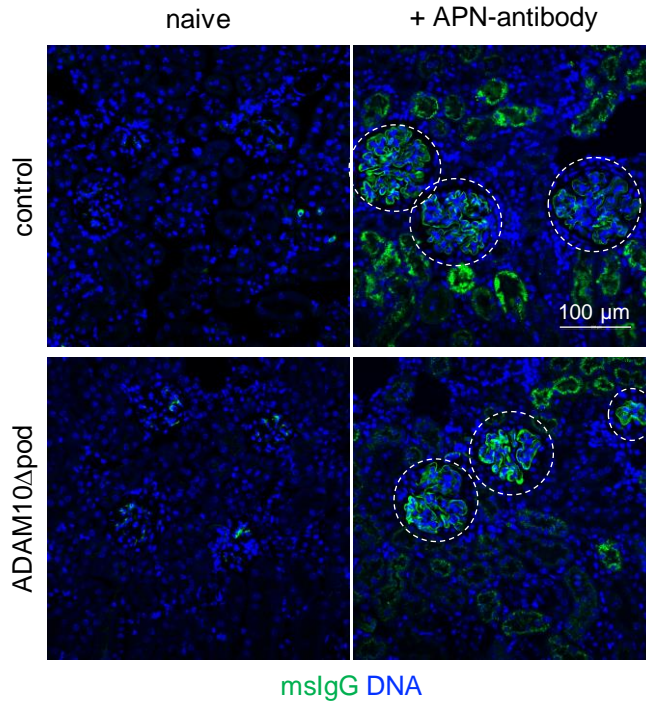
Supplementary Figure 3: ADAM10 localization in human glomerular injuries. Overview and close-ups of ADAM10 expression in patients using an antibody to ADAM10 (rb- α -ADAM10, Pineda, antigen retrieval protease 24), lectin wheat germ agglutinin (WGA, red), and DNA (Hoechst, blue). An n=4 biopsies per disease entity were analyzed, a representative glomerulus is shown: diabetic nephropathy (DN), ANCA positive rapid progressive glomerulonephritis (ANCA + RPGN), anti-GBM glomerulonephritis (anti-GBM GN), membranous nephropathy (MN), focal segmental glomerulosclerosis (FSGS), minimal change disease (MCD). Green arrows: ADAM10 expression at the endothelial side of the glomerular filtration barrier, white arrows: ADAM10 expression at the podocyte aspect of the glomerular filtration barrier.

A**B**

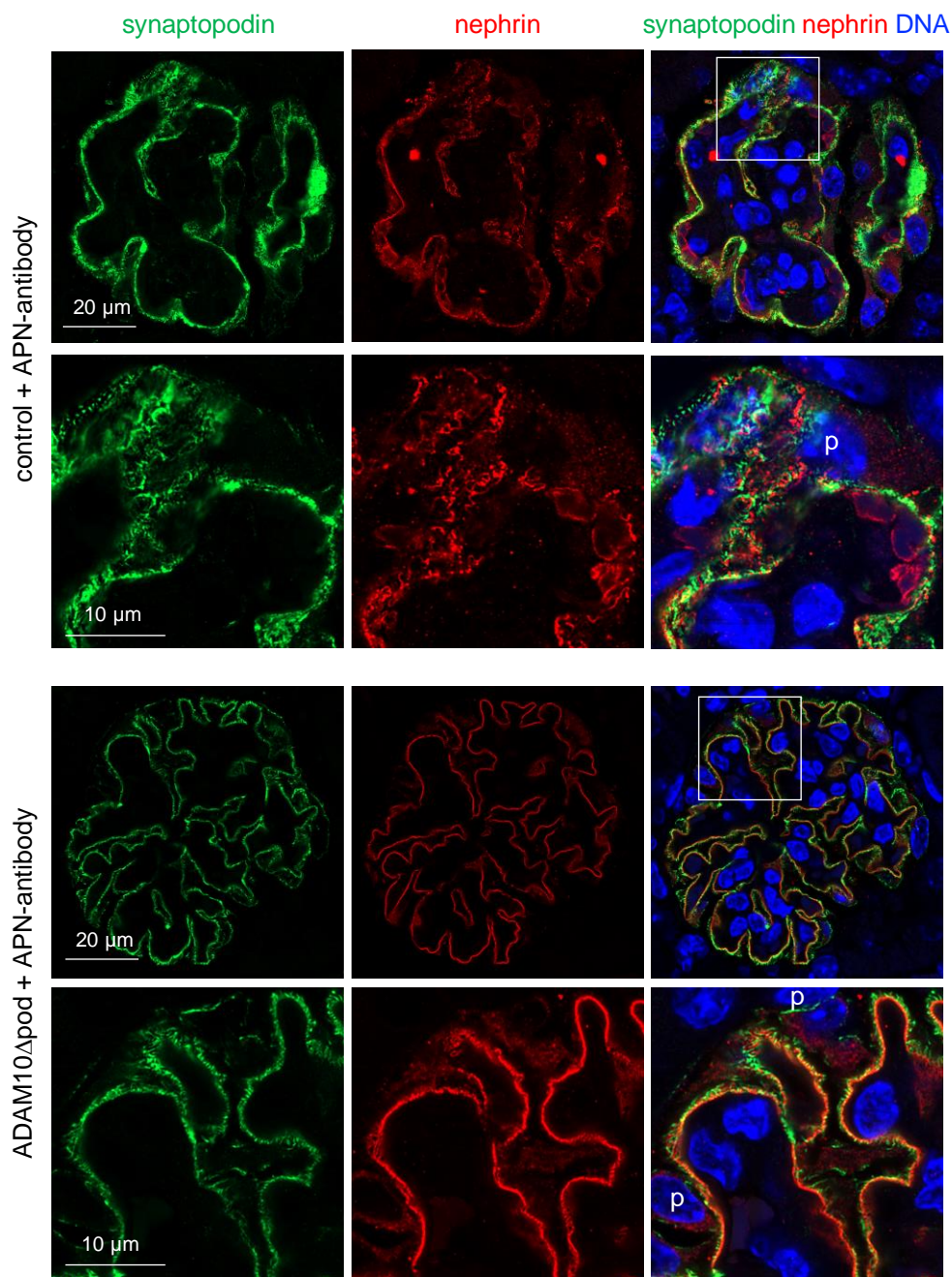
Supplementary Figure 4: Glomerular ADAM10 expression increases in APN. Anti-podocyte nephritis was induced in C57BL/6 mice. Kidneys were analyzed on day 14. Representative confocal images of (A) cryosections demonstrating ADAM10 (green) expression in relation to the slit diaphragm protein nephrin (red), and DNA (blue, Hoechst) using a rat anti-ADAM10 antibody. Representative confocal images of (B) paraffin sections demonstrating podocyte (p) ADAM10 (green) expression in relation to the slit diaphragm protein nephrin (red), wheat germ agglutinin to demarcate the glycocalyx (WGA, light blue), and DNA (white, Hoechst) using a rabbit anti-ADAM10 antibody. White arrows point towards glomerular endothelial ADAM10 expression.



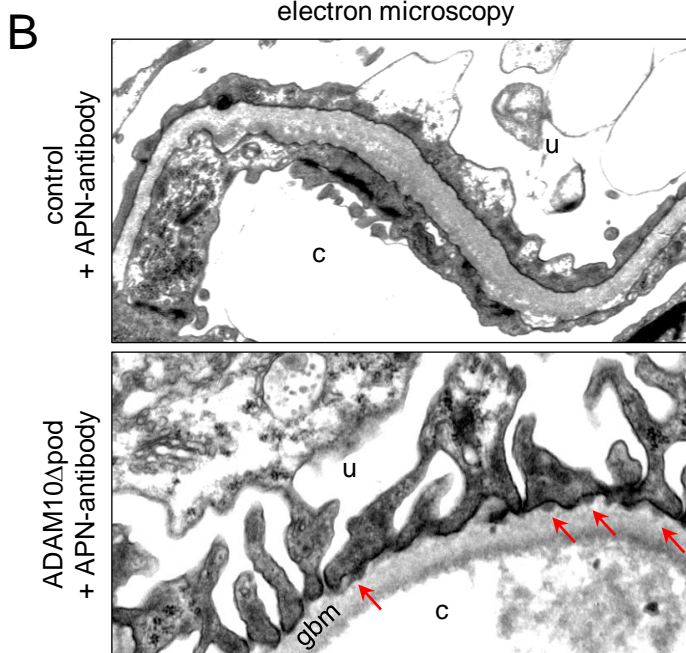
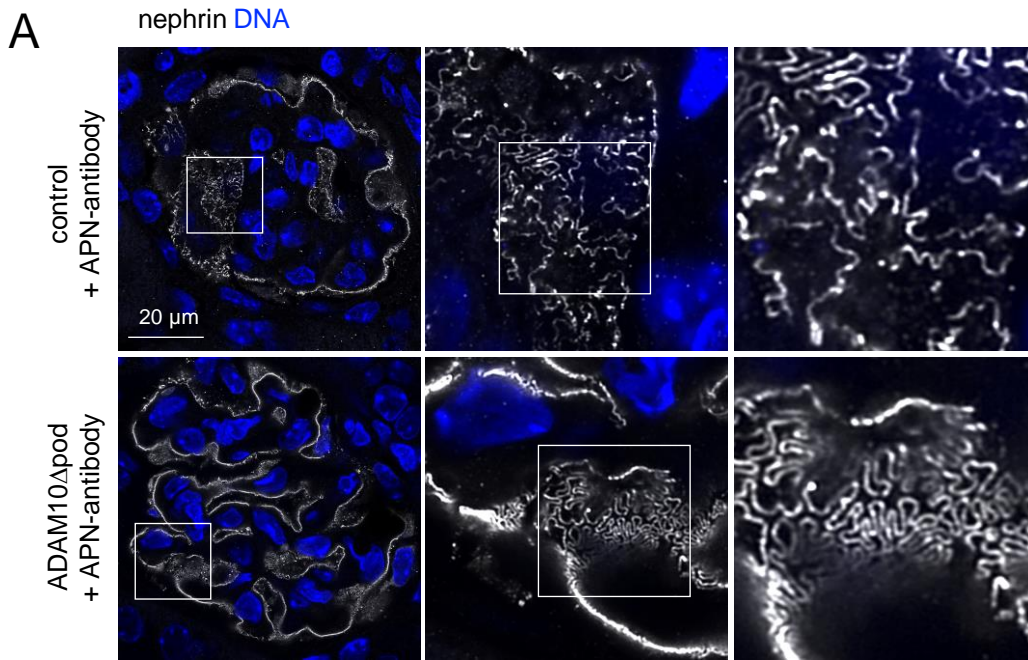
Supplementary Figure 5: Alteration of glomerular morphology is attenuated in APN antibody treated ADAM10 Δ pod mice. Anti-podocyte nephritis was induced in ADAM10 Δ pod and control littermates. Kidneys were analyzed on day 14. Representative light micrographs of Periodic Acid Schiff (PAS) staining exhibiting the tubulointerstitial and glomerular morphology. Note the comparable occurrence of PAS-positive protein casts in the tubular lumina (asterisks) of ADAM10 Δ pod and control littermate mice, contrasting the preserved glomerular morphology in ADAM10 Δ pod mice. The visible brown round structures represent the perfused magnetic beads used for glomerular isolation.



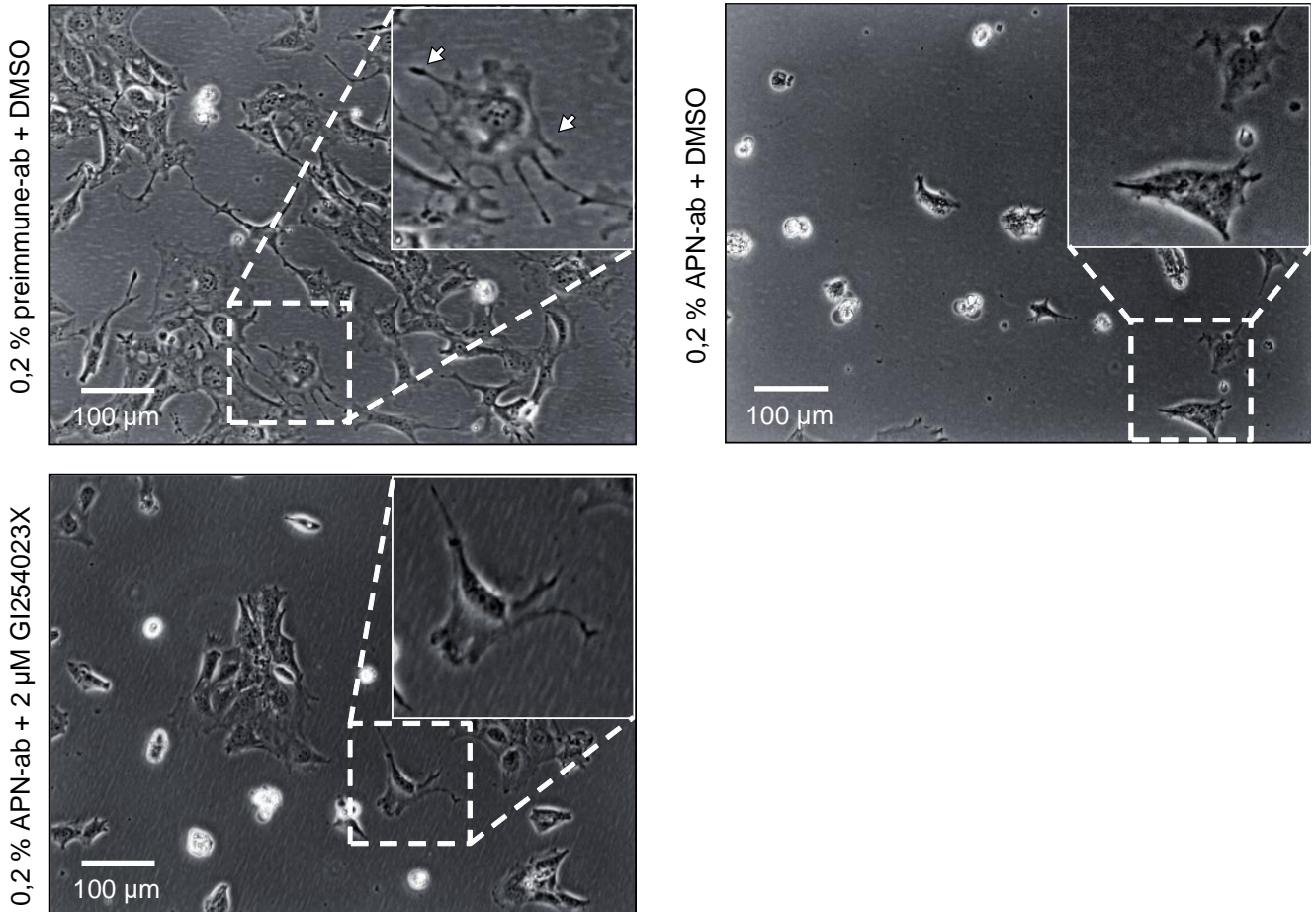
Supplementary Figure 6: Intrinsic mouse IgG deposition does not differ between ADAM10 Δ pod and control littermate mice in APN. Anti-podocyte nephritis was induced in ADAM10 Δ pod and control littermates. Kidneys were analyzed on day 14. Representative confocal images of the mouse IgG (green) demonstrate similar staining intensity for mslgG in glomeruli (highlighted through dashed circle) of both genotypes, DNA (blue, Hoechst).



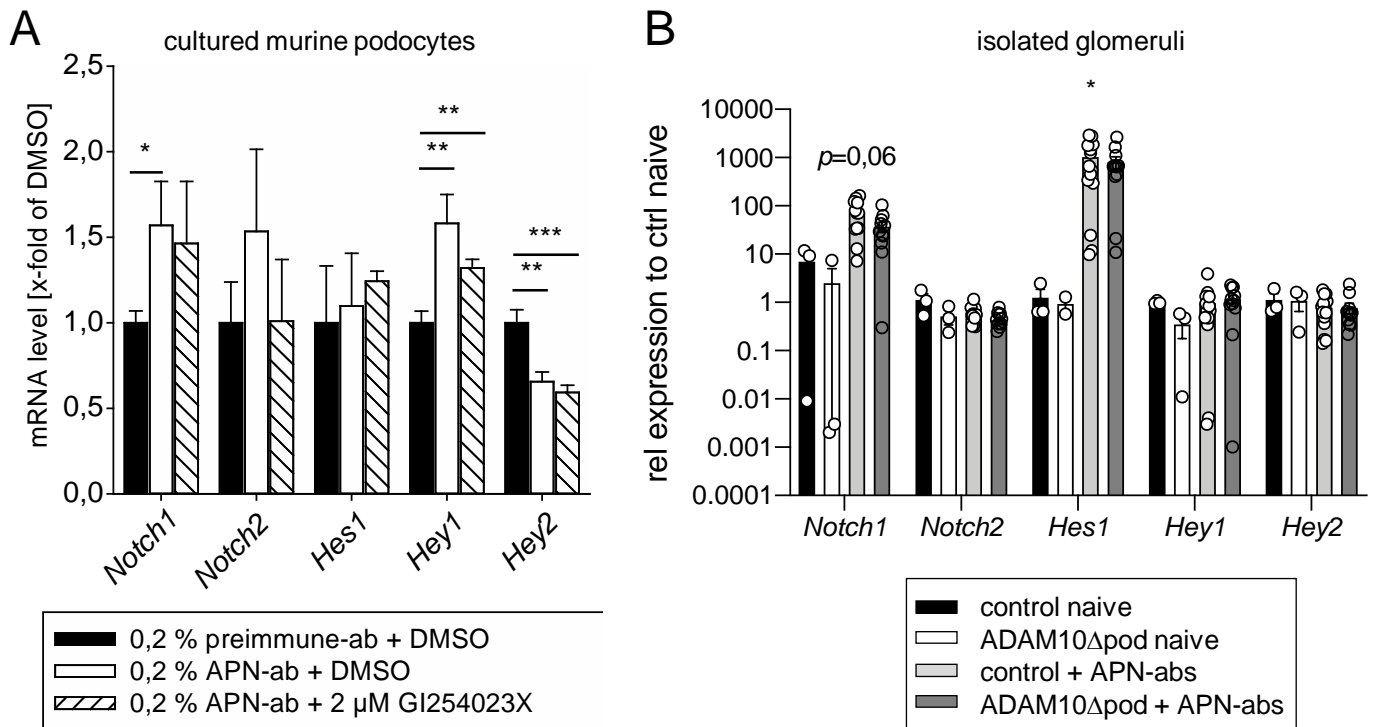
Supplementary Figure 7: Alteration of podocyte structure is attenuated in ADAM10 Δ pod mice in APN. Anti-podocyte nephritis was induced in ADAM10 Δ pod and control littermates. Kidneys were analyzed on day 14. Representative high-resolution confocal images of the actin-regulating foot process protein synaptopodin (green) and the slit diaphragm protein nephrin (red), DNA (blue, Hoechst) expression in podocytes (p). Note the mostly preserved immunolocalization of both proteins in ADAM10 Δ pod mice.



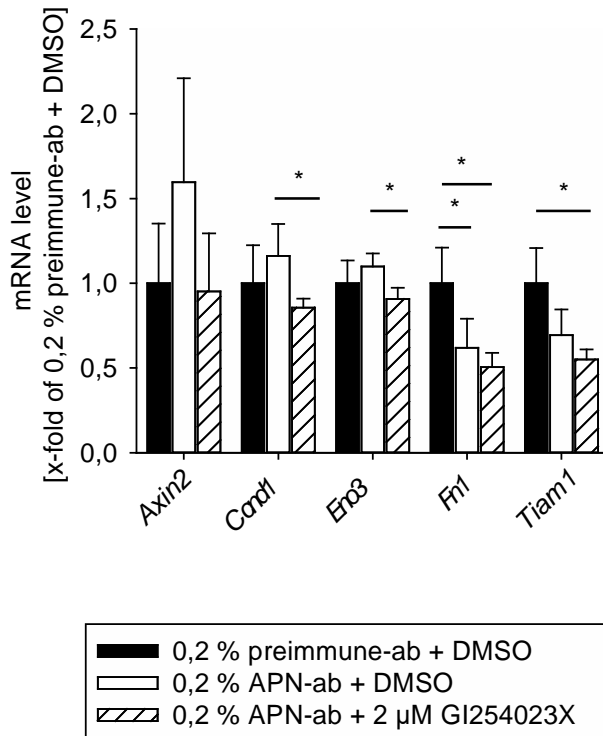
Supplementary Figure 8: Foot process effacement is attenuated in ADAM10 Δ pod mice in APN nephritis. Anti-podocyte nephritis was induced in ADAM10 Δ pod and control littermates. Kidneys were analyzed on day 14. **(A)** Representative high-resolution confocal images of the distribution of nephrin (white) at the slit diaphragm (meandering white line) exhibits massive foot process effacement in control mice in contrast to areas of foot process broadening in ADAM10 Δ pod mice. DNA (blue) is visualized by Hoechst staining. **(B)** Ultrastructural analysis of podocytes demonstrates foot process effacement in control mice upon APN-antibody treatment, while ADAM10-deficient podocytes are morphological mostly preserved, even those overlying electron dense subepithelial deposits (red arrows). Scale bars = 500 nm; c = capillary lumen, u = urinary side, gbm = glomerular basement membrane.



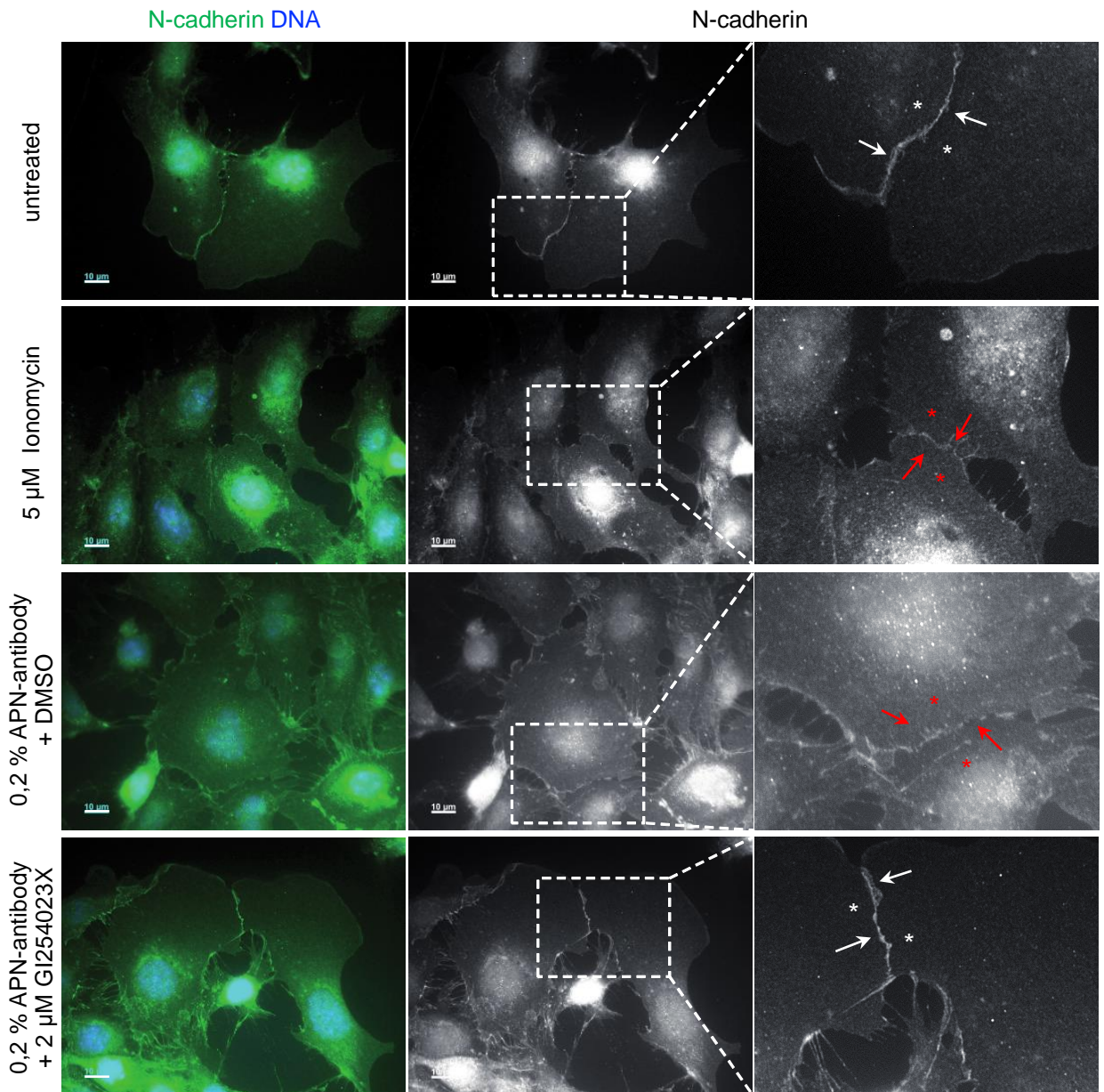
Supplementary Figure 9: Cultured murine podocytes exposed to APN antibodies represent a suitable model for the analysis of ADAM10 function. Murine podocytes were exposed for 24-hours to APN antibodies or to control pre-immune antibodies with or without the ADAM10 inhibitor GI254023X. Podocytes respond to APN-antibody by cell process retraction and cell body condensation. Incubation with the ADAM10 inhibitor GI254023X was sufficient to partially rescue the morphological changes. Scale bars = 100 μm .



Supplementary Figure 10: The Notch signaling pathway is not activated in an ADAM10-dependent way in podocytes after exposure to APN-antibodies. (A) Murine podocytes were exposed for 24-hours to APN antibodies or to control pre-immune antibodies with or without the ADAM10 inhibitor GI254023X. DMSO was used as vehicle. qRT-PCR analysis on *Notch* expression and Notch-response genes argues against a contribution of Notch signalling to podocyte injury. Only *Hey1* is significantly increased upon APN-induction and suppressed with GI254023X, which however can also be attributed to Notch-independent signalling pathways. 4 replicates for each condition were evaluated and compared to pre-immune antibody and DMSO treated podocytes. * $p \leq 0.05$, ** $p \leq 0.01$, *** $p \leq 0.01$. (B) Anti-podocyte nephritis was induced in ADAM10 Δ pod and control littermates. Glomerular transcript levels for Notch-response genes were analyzed on day 14, * $p \leq 0.05$ to control (ctrl) naïve, n = 3-14, pooled data of two independent experiments.

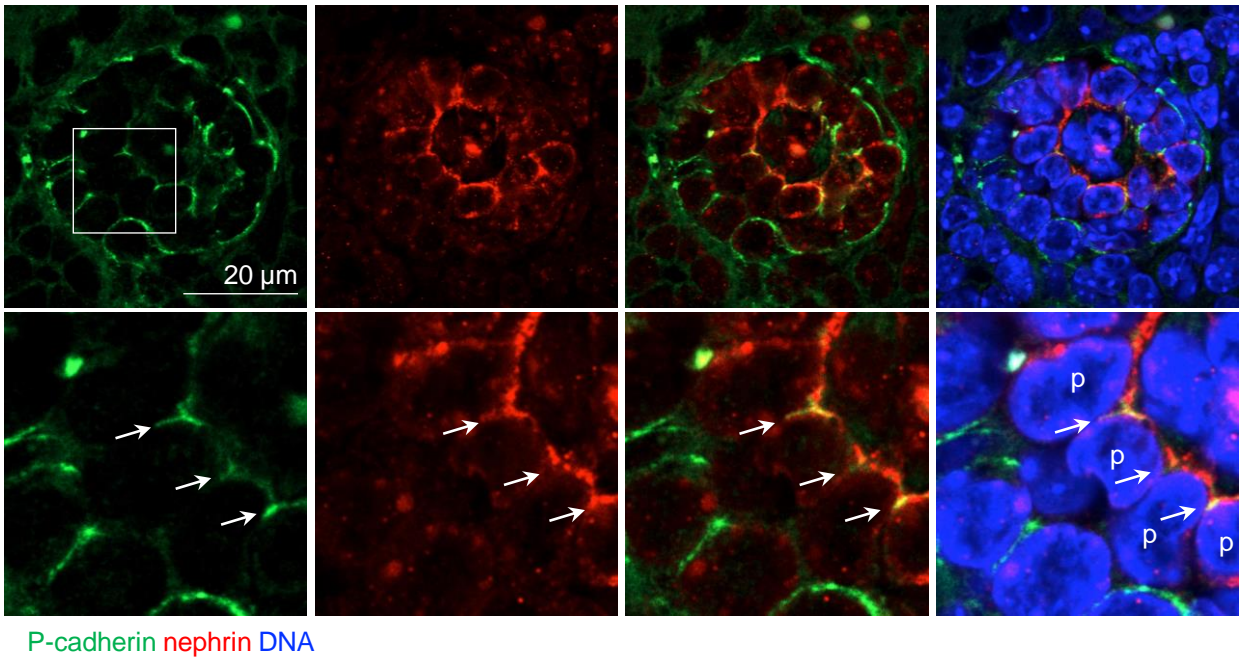


Supplementary Figure 11: Activation of Wnt signaling pathways after exposure to APN-antibodies partially depends on ADAM10 in podocytes. Murine podocytes were exposed for 24-hours to APN antibodies or to control pre-immune antibodies with or without the ADAM10 inhibitor GI254023X. DMSO was used as vehicle. qRT-PCR analysis suggests an ADAM10-dependent stimulation of Wnt-response genes upon APN-antibody treatment as manifested by a significant increase in *Ccnd1* and *Eno3* expression, which is abrogated by the ADAM10 inhibitor GI254023X. Wnt-response genes *Fn1* and *Tiam1* are spared from transcriptional effects. 4 replicates for each condition were evaluated, * $p \leq 0.05$.

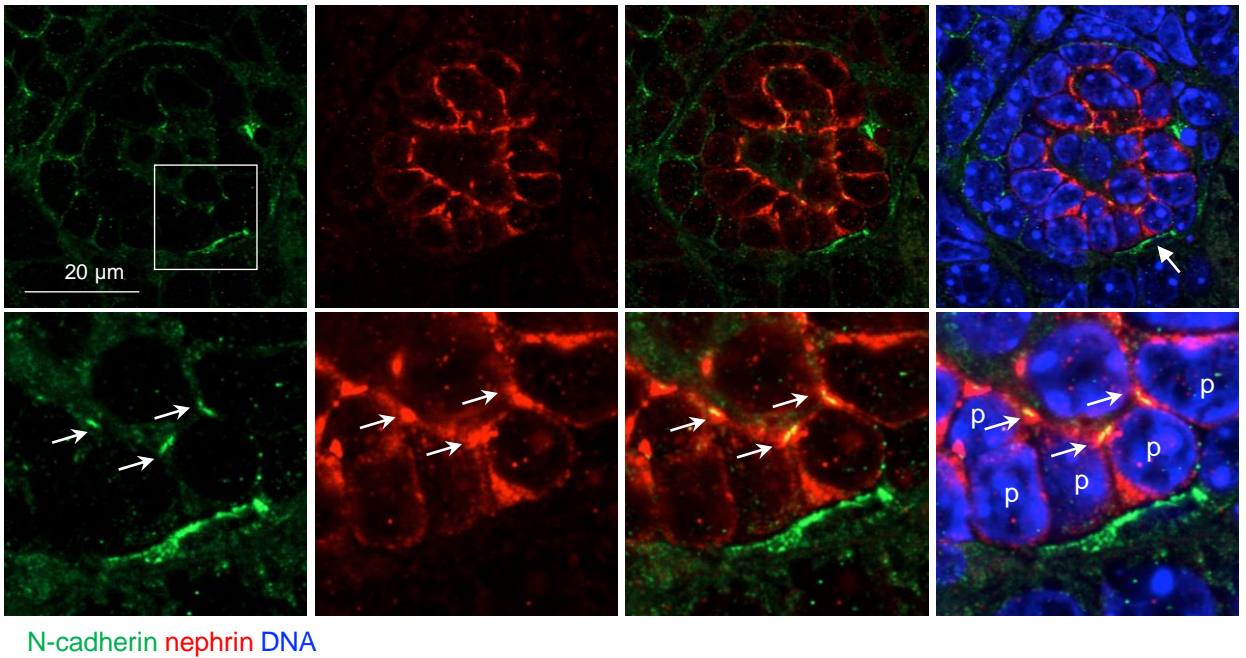


Supplementary Figure 12: N-cadherin is shed in an ADAM10-dependent manner in cultured murine podocytes. Fluorescence images of untreated cultured murine podocytes reveals N-cadherin localization primarily at cell-cell-contact sites (white arrows), while signal at non-contacting areas (white asterisks) is weak. Treatment with the ADAM10 activator Ionomycin, suppresses N-cadherin staining at cell-cell contact sites (red arrows) to amounts of cytoplasmic N-cadherin signal (red asterisks), presumably due to increased shedding activity. Application of the APN-antibody yielded an outcome similar to Ionomycin treatment, since again the difference between cell-cell contact and cytoplasmic N-cadherin staining was reduced. Finally, inhibition of ADAM10 activity with GI254023X could rescue N-cadherin surface expression at cell-cell contacts of APN-antibody exposed podocytes (white arrows), proving APN-induced shedding of cell-adhesion molecules by ADAM10.

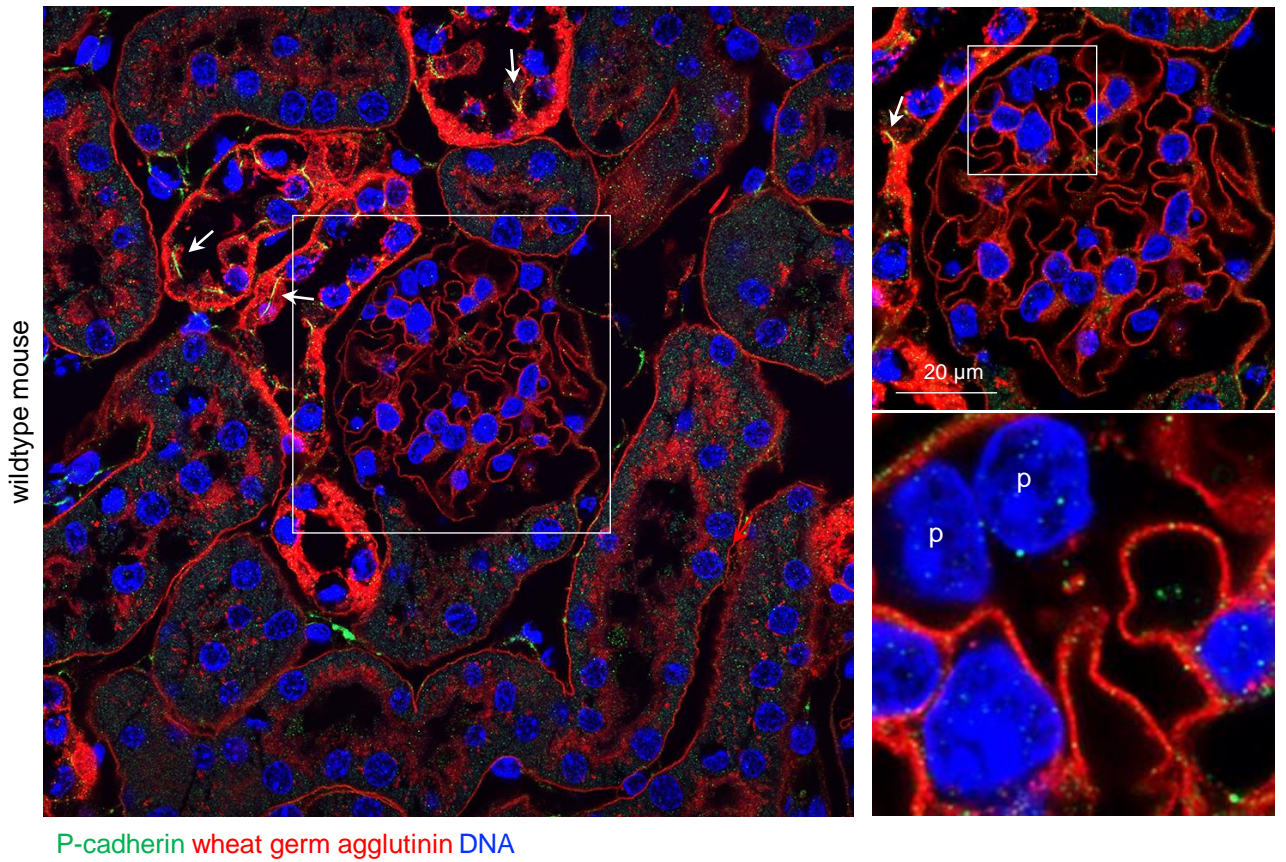
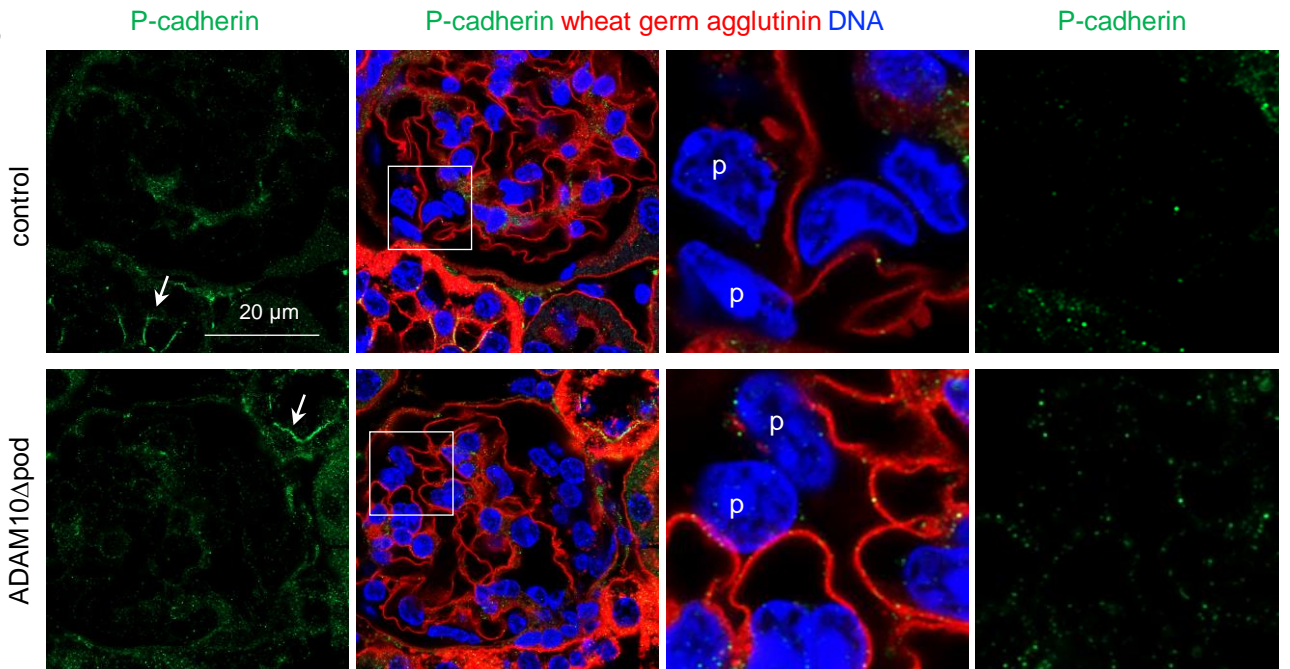
A



B

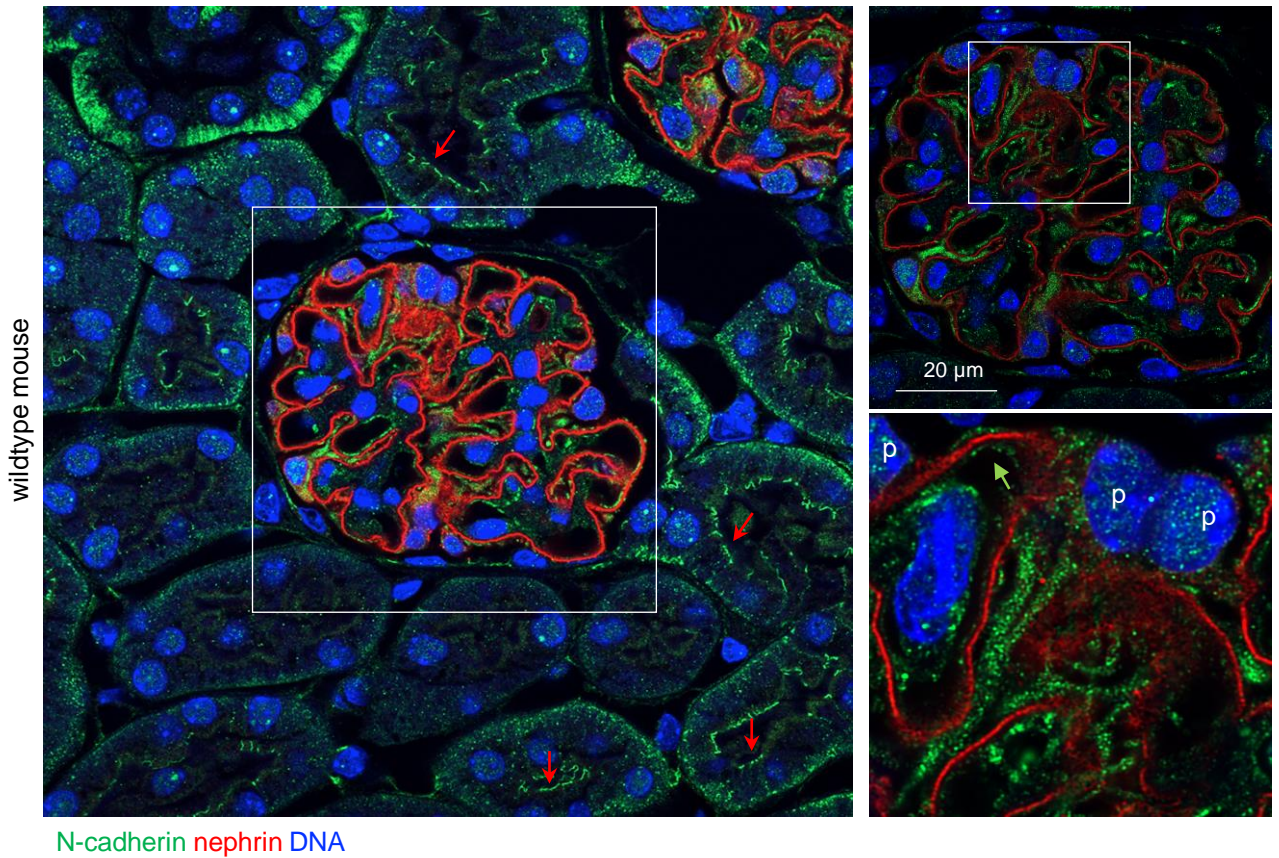


Supplementary Figure 13: Cell-cell adhesion proteins are expressed at the apical side of developing podocytes. Representative high-resolution confocal microscopy of postnatal day 5 C57BL/6 mouse kidneys for the cell-cell adhesion protein P-cadherin (A) and (B) N-cadherin (both green) in relation to the slit diaphragm protein nephrin (red) and DNA (blue, Hoechst). White arrows point towards co-localization of P- or N-cadherin with nephrin at the apical aspect of developing podocytes (p) at the capillary phase of glomerular development.

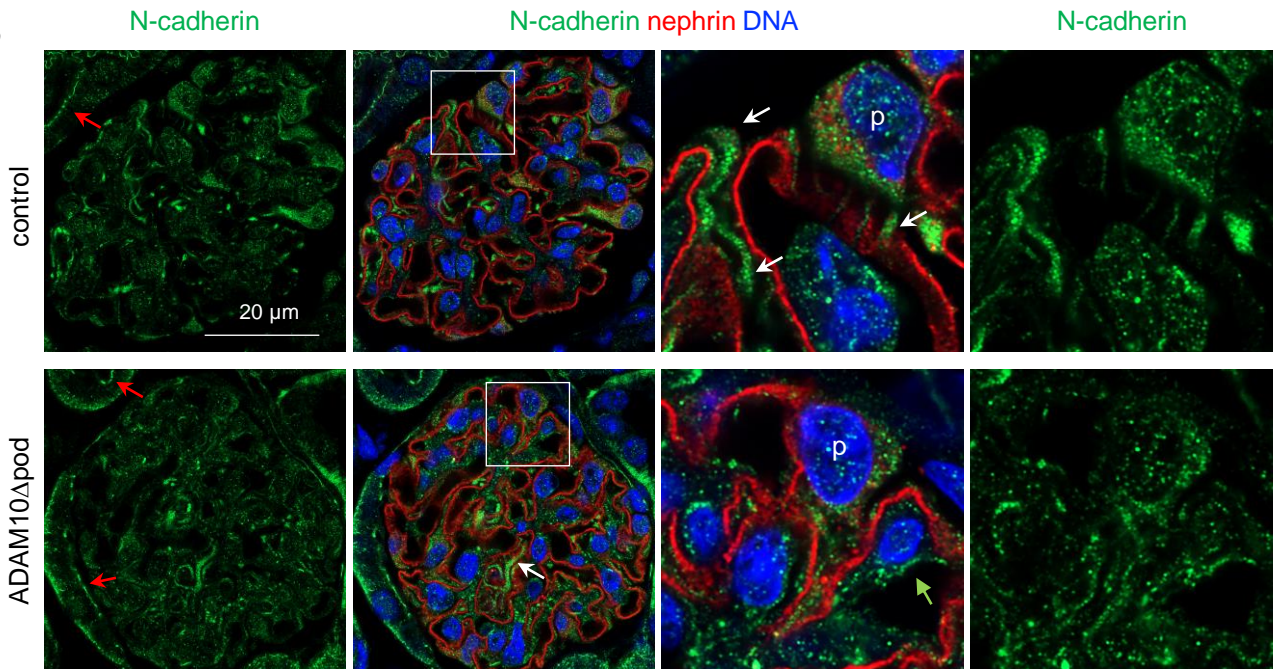
A**B**

Supplementary Figure 14: P-cadherin expression does not differ between naive ADAM10 Δ pod and control littermate mice. Representative high-resolution confocal microscopy of renal and podocyte (p) P-cadherin (green) expression in relation to the lectin wheat germ agglutinin (red) and DNA (blue, Hoechst) in **(A)** C57BL/6 wildtype mouse and **(B)** ADAM10 Δ pod and control littermate mice. No clear podocyte expression was seen. Note the strong and apical expression of P-cadherin in tubular cells (white arrows).

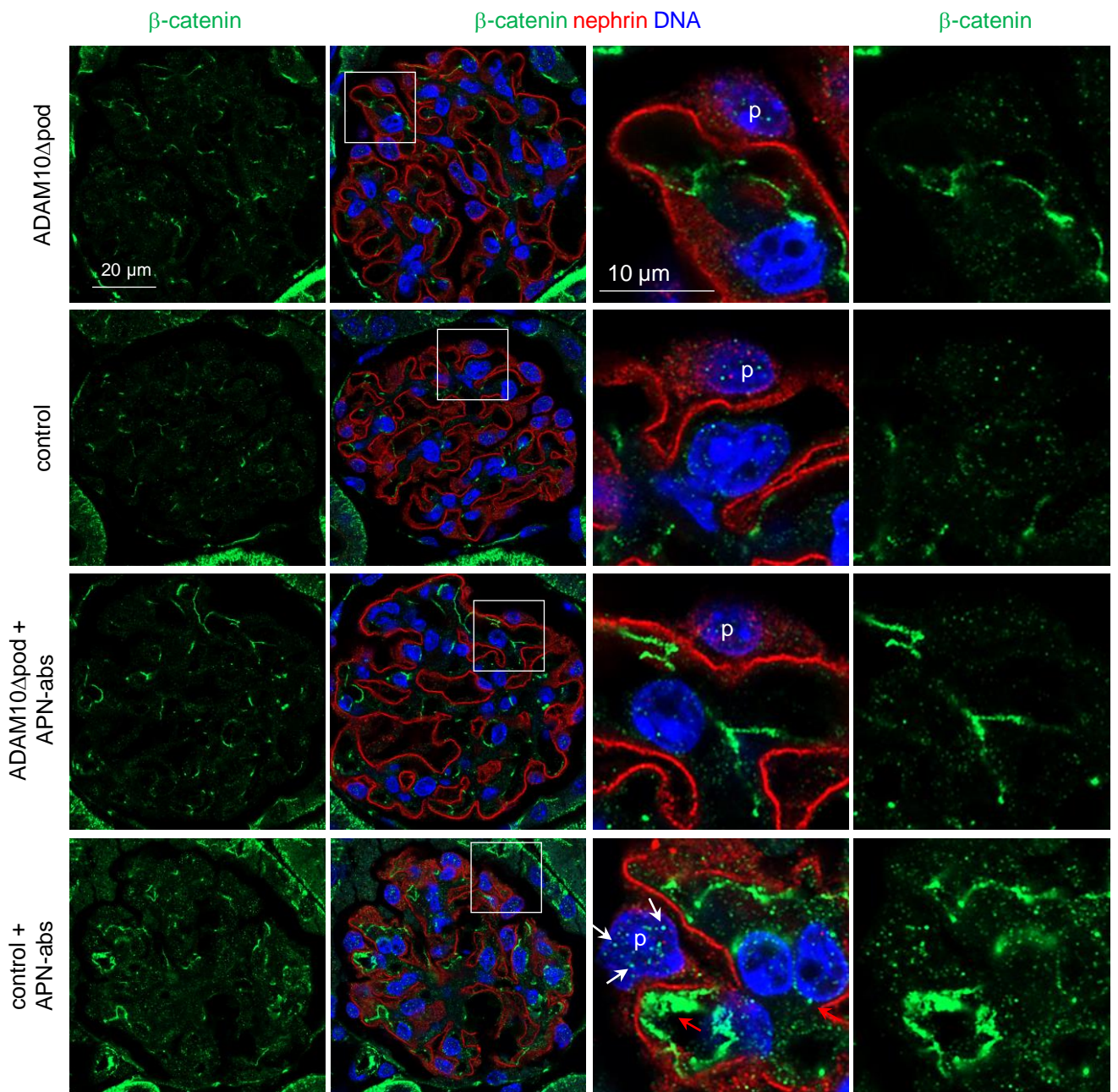
A



B



Supplementary Figure 15: N-cadherin expression does not differ between naive ADAM10 Δ pod and control littermate mice. Representative high-resolution confocal microscopy of renal and podocyte (p) N-cadherin (green) expression in relation to the slit diaphragm cell-cell adhesion protein nephrin (red) and DNA (blue, Hoechst) in (A) C57BL/6 wildtype mouse and (B) ADAM10 Δ pod and control littermate mice. High N-cadherin antibody concentrations were used to visualize a podocyte expression. Note the strong and apical expression of N-cadherin in tubular cells (red arrows). In podocytes, N-cadherin is found in the cytoplasm and in primary processes (white arrows) and in glomerular endothelial cells (green arrows).



Supplementary Figure 16: β -catenin expression is enhanced in the nuclei and cytoplasm of podocytes in the setting of APN nephritis. Kidneys from APN antibody exposed ADAM10 Δ pod and control littermates on day 14 were stained for β -catenin (green) in relation to the slit diaphragm protein nephrin (red) and DNA (blue, Draq5). Representative confocal images demonstrate enhanced glomerular expression of β -catenin in the podocyte (p) cytoplasm and nuclei (white arrows) of an APN treated control mouse in comparison to APN treated ADAM10 Δ pod podocytes. A prominent expression of β -catenin was noted in the cytoplasm of glomerular endothelial cells.

gene	Primer forward sequence	Primer reverse sequence
<i>Adam10</i>	5' GGAAGAAATGCAAGCTGAA	5' CTGTACAGCAGGGTCCTTGAC
<i>Axin2</i>	5' GAGAGTGAGCGGCAGAGC	5' CGGCTGACTCGTTCTCCT
<i>Ccnd1</i>	5' TTTCTTTCCAGAGTCATCAAGTGT	5' TGACTCCAGAAGGGCTTCAA
<i>Fn1</i>	5' CGGAGAGAGTGCCCCTACTA	5' CGATATTGGTGAATCGCAGA
<i>Hes1</i>	5' TGCCAGCATGATATAATGGAGAA	5' CCATGATAGGCTTTGATGACTTT
<i>Hey1</i>	5' CATGAAGAGAGCTCACCCAGA	5' GAACACAGAGCCGAACTCAA
<i>Hey2</i>	5' GTGGGGAGCGAGAACAATTA	5' GTTGTCGGTGAATTGGACCT
<i>Notch1</i>	5' CTGGACCCCATGGACATC	5' AGGATGACTGCACACATTGC
<i>Notch2</i>	5' TGCCTGTTTGACAACCTTTGAGT	5' GTGGTCTGCACAGTATTTGTCAT
<i>Tiam1</i>	5' GGAATATTTGATGACACTGTTCCA	5' GGTGGACACTGGGTAAGACC
<i>Tuba1a</i>	5' CTGGAACCCACGGTCATC	5' GTGGCCACGAGCATAGTTATT
<i>Eno3</i>	5' CAGATCTTGAGGCAATCC	5' CCGCCGTTGATCACATTA
<i>18S</i>	5' CACGGCCGGTACAGTGAAAC	5' AGAGGAGCGAGCGACCAAA

Supplementary Table 1: Oligonucleotide sequences for used for qRT-PCR in cultured murine podocytes and isolated glomeruli.

Protein	Glomerular membrane preparation	Cell-type specific proteome
<i>Inhibitors</i>		
Timp1	Not detected	Not detected
Timp3	Detected 27	Not detected
<i>Sheddases</i>		
Adam9	Detected 27	Not detected
Adam15	Detected in one mouse 24	Not detected
Meprin β	Detected 27	Not detected
<i>Tetraspanins</i>		
Tspan15	28	More in PC, less in GEnC
Tspan14	28	More in GEnC
Tspan5	27	More in PC, less in GEnC and MC
Tspan33	Detected in one mouse 22	Not detected
Tspan17	Not detected	Not detected
Tspan10	Not detected	Not detected
Tspan3	Not detected	Not detected
Tspan12	Not detected	Not detected
<i>Transport proteins</i>		
Ap2a1	Detected 30	More in PC, less in GEnC and MC
Ap2a2	Detected 31	More in GEnC
Ap2b1	Detected 31	More in GEnC, less in PC
Ap2m1	Detected 30	More in PC, less in MC
Ap2s1	Detected 29	Similar amounts in all glomerular cell types
SAP97/Dlg1	Detected 29	More in PC, less in GEnC

Supplementary Table 2: Summary of the findings regarding ADAM10 regulators in our proteomic datasets. For proteins relevant to Adam10 regulation, information about the detection in our proteomics analysis is given. For the glomerular membrane dataset, LFQ intensity is indicated, whereas for the dataset on isolated glomerular cell types, observed significant differences between cell types are specified. The proteomic analysis of sorted glomerular cells exhibit an expression of AP2 subunits and SAP97/Dlg1 in all three glomerular cell types, both being relevant for Adam10 trafficking and recycling. Three relevant tetraspanins (Tspans) are differentially expressed among glomerular cells, indicating a potential cell-type specific regulation of ADAM10 activity and/or substrate specificity. Tspan15 has been described to inhibit Adam10-mediated notch activation upon ligand binding. Its expression possibly represents reduced dependence of podocytes on notch signaling and could potentially explain the lack of podocyte development defects we observed in ADAM10 Δ pod mice. Furthermore, Tspan15 mediates ADAM10 dependent shedding of N-Cadherin by fostering its transport to the cell surface. Tspan5, on the other hand, is involved in site-specific proteolysis of CD44 by ADAM10, a receptor facilitating cell-matrix interaction (<https://doi.org/10.1007/s00018-015-2111-z>). Proteomic data generated by mass spectrometric analysis of membrane fractions from isolated whole mouse glomeruli. Three proteins that were not detected in our dataset based on sorted glomerular cells are robustly detected here: TIMP3, ADAM9 and Meprin β . TIMP3 has been described that it can act on cells that do not produce TIMP3 themselves (<https://doi.org/10.1016/j.ejvs.2017.07.002>).